Gravity-induced collapse of a soft rock cliff due to notch growth

**Submitted:** 06 April 2024

**Published online in 'accepted manuscript' format:** 26 September 2024

**Manuscript title:** Gravity-induced collapse of a soft rock cliff due to notch growth

**Authors:** Maria Lia Napoli[1], Monica Barbero[1], F. Mascioli[2] and E. Miccadei[3]

**Affiliations:** [1]Department of Structural, Geotechnical and Building Engineering, Politecnico di Torino, C.so Duca degli Abruzzi 24, 10124, Torino, Italy, [2]NLWKN-Coastal Research Station/Forschungsstelle Küste, Jahnstraße 1, 26506 Norden, Germany, [3]Department of Engineering and Geology, Università degli Studi "G. d'Annunzio" Chieti-Pescara, Laboratory of Tectonic

**Corresponding author:** Maria Lia Napoli, Department of Structural, Geotechnical and Building Engineering, Politecnico di Torino, C.so Duca degli Abruzzi 24, 10124, Torino, Italy

**E-mail:** maria.napoli@polito.it

Accepted manuscript doi:
10.1680/jenge.24.00052

**Abstract**

Cliff erosion is an unstoppable natural process increasingly occurring due to climate change and frequently causing crucial georisks on rocky coasts throughout the world. The resilience of a cliff depends on a variety of environmental, geometrical, geological and geotechnical conditions that have been included in several heuristic coastal hazard assessment approaches. In order to provide new quantitative insights into the relationship between some geometrical and structural characteristics of a sea cliff (height, basal erosion, discontinuities) and its stability conditions (failure mechanism, safety factor) this paper investigates numerically how the progressive undermining of a soft rock cliff affects its mechanical behaviour. It has been found that the undermining depth plays a significant role on cliff stability, whose mechanism of collapse changes according to the overhang slenderness. When a vertical joint is present, the higher is its persistence the lower is the global safety factor. Moreover, as the joint moves away from the cliff face the safety factor decreases, the worse condition being found when it is above the notch end. The results obtained can contribute to a deeper understanding of the failure mechanisms of seacliffs, helping in a reliable assessment of coastal risk and a proper design of the mitigation measures

**Keywords:** cliff erosion, climate change, coastal hazard assessment, notch, numerical modelling, soft rocks

Accepted manuscript doi:
10.1680/jenge.24.00052

## Introduction

Cliff erosion and retreat processes are due to marine, sub-aerial and anthropogenic processes such as hydrodynamic impact of wind-induced sea waves, nearshore current actions, reduction of rock strength by weathering, sea spray, long-term sea-level rise, loss of defensive beaches and removal of protective fallen debris from the lower seacliff face (Naylor and Stephenson, 2010; Kline, Adams and Limber, 2014; Sunamura, 2015; Castedo *et al.*, 2017; Dodge-Wan, D. Nagarajan, 2019; Miccadei *et al.*, 2019; Young *et al.*, 2021). Due to climate change and global warming these factors are escalating in frequency and intensity in recent decades (Bray and Hooke, 1997; Dickson, Walkden and Hall, 2007; Bonaldo *et al.*, 2019; Theodore *et al.*, 2020; Gómez-Pazo, Pérez-Alberti and Trenhaile, 2021; Lollino *et al.*, 2021; Pang *et al.*, 2023). As a consequence, the occurrence and severity of coastal erosion-induced landslides (often caused by the growth of cliff notches) and the associated losses of coastal land and properties have significantly increased (Duperret *et al.*, 2004; Kogure *et al.*, 2006; Wolters and Gerald, 2008; Young and Ashford, 2008; Budetta, 2011; Andriani and Pellegrini, 2014; Ružić *et al.*, 2015; Young, 2018; Theodore *et al.*, 2020; Zhang *et al.*, 2023), becoming a serious challenge for many coastal communities that are not resilient enough to extreme weather events.

In the last decades, several coastal hazard assessment approaches have been proposed all over the world to support decision-making in coastal risk management and land-use planning (De Pippo *et al.*, 2008; Del Río and Gracia, 2009; Nunes *et al.*, 2009; Marques, Matildes and Redweik, 2011; Marques, 2018; Gerivani, Stephenson and Afarin, 2020). Most of these approaches, through the weighting and combination of selected geometrical, environmental,

geological and structural factors (considered the main responsible for cliff instability), provide a Hazard Index that can be used to generate hazard maps. However it is worth pointing out that most of these approaches i) are site-specific (e.g., the prediction of the most critical rock cliff stretches are based on factors that affected past collapses in a specific coastal environment); ii) are affected by a certain degree of subjectivity (e.g., heuristic approaches, that are based on expert opinions both in the selection of the main factors responsible for cliff instabilities, and in their weighting); and (iii) the influence of basal erosion has been rarely taken into account (although its presence has been widely recognized as a significant contributing factor to cliff collapse (Sunamura, 1975, 2015; Kogure *et al.*, 2006; Budetta, 2011; Castedo *et al.*, 2017; Lollino *et al.*, 2018; Theodore *et al.*, 2020)).

Since retreat rates of soft rock coasts are up to two orders of magnitude greater than hard rock cliffs (Budetta, Santo and Vivenzio, 2008; Miccadei *et al.*, 2019), this research investigates numerically, through a parametric analysis, how the stability of soft rock cliffs with variable geometrical and structural configurations is affected by the presence of a basal notch.

First, 2D finite element (FE) analyses were carried out on homogeneous steep seacliffs with variable heights (from 7 m up to 25 m) and the same basal notch, to investigate if and how the slenderness of the rock overhangs affects their failure mechanism. The geometry and the mechanical properties of the cliff were based on the study of Calista et al. (2019) and Miccadei et al. (2019), related to the popular tourist site of Punta Ferruccio promontory, located in the Adriatic Sea (Abruzzo, Italy), which has been affected by several rockfalls in the last decades (Figure 1).

Then, a back analysis of the 2014 rockfall event occurred in that site was performed. The Punta Ferruccio promontory is mainly composed of conglomerate (including clayey and sandstone lenses) with structural vertical joints spaced from 3 m to 10 m, and is affected by some deep notches at its base. In this paper, to study the failure mechanism of the promontory, a vertical joint above the maximum notch depth in the 25 m high homogeneous model was introduced. Since one of the most difficult parameters to estimate is the persistence of the joints, a parametric analysis was carried out to determine the critical joint persistence that provided a safety factor close to 1 (i.e. incipient collapse condition). From such analysis some considerations were made on the influence of a variably persistent joint on the stability of a cliff.

Finally, the 2014 back-analysed Punta Ferruccio model was modified by locating the joint at different distances from the cliff face, to also investigate how the stability of a cliff is influenced by the joint position.

The results obtained can contribute to a deeper understanding of the failure mechanisms of rocky coasts, giving higher reliability to coastal hazard and risk assessment and essential information for a proper design of the mitigation measures.

## Stability of homogeneous soft rock cliffs with basal erosion

In order to study the effects of basal erosion on the stability of plunging cliffs in homogeneous soft rocks in the absence of structural rock joints, 2D FEM stability analyses were performed with the software RS2 (vers. 11.010) from Rocscience. Rock cliffs with a basal notch 7 m deep ($L_n$) and 4 m high ($h_n$) and variable heights ($H_c$), from 7 m up to 25 m, were considered. Six-

node triangular elements were used to mesh the models, increasing the elements density close to the cliff face and the notch. In order to avoid stress modelling disturbance, two excavation processes (i.e. each one including several excavation stages) were simulated: the former in the left part of the model so as to reproduce the vertical cliff face, with a removal of 2.5 m layers of rock per stage; the second, in order to simulate the notch growth and its effect on the stability of the cliff, with a removal of 1 m of notch depth per stage (Figure 2).

The mechanical parameters of the rock have been taken from a previous study by Calista et al. (2019), and are reported in Table 1. A linear elastic-perfectly plastic Mohr-Coulomb behaviour was assigned to the rock mass.

The effect of the notch growth is shown in Figure 3 and Figure 4 in terms of maximum shear strains and yielded elements for the highest ($H_c$=25 m) and lowest ($H_c$=7 m) cliffs analysed, respectively. From these figures, there is compelling evidence that the presence of a basal notch causes shear concentrations close to the erosion region, and that their magnitude depends on the erosion deep, whatever the height of the cliff. However, by comparing Figure 3 and Figure 4, a different behaviour can be observed between the two cliff types: the highest cliff presents from the first excavation stage (Figure 3a, $L_n$ = 1 m) several yielded elements (localized shear failure). When the notch grows, a significant increment of yielded elements appears, but such elements are all located on (or very close to) the notch contour, while no effect on the surface is detected yet. On the contrary, as shown in Figure 4, the lowest cliff starts presenting yielded elements when the notch depth is 5 m (Figure 4e, $L_n$ = 5 m). Moreover, when the notch deepens further

Accepted manuscript doi:
10.1680/jenge.24.00052

(Figure 4f-g, $L_n$= 6-7 m), a significant area of the rock mass located on the top of the cliff experiences yielding (shear and tensile failure).

The Shear Strength Reduction technique (SSR), involving progressive reductions in the shear strength of the rock, was used in order to compute the critical (Strength Reduction) factor at which failure occurs (SRF), i.e. the global safety factor (SF) of the cliff, and to visualize the failure mechanisms. The SRFs obtained are listed in Table 2.

Figure 5 shows the maximum shear strains, total displacements and yielded elements at failure (i.e. at critical SRF) of the 25m and 7m high models. It is evident that shear strains develop from the notch (Figure 3 and Figure 4) and propagate upwards, and that tensile failure is generated at the top of the cliff. This result indicates that tension cracks can be originated both in high and low seacliffs, due to the detrimental effect of a basal erosion, as commonly observed just behind the crest of steep cliffs, and found from previous findings from the literature (Kogure *et al.*, 2006; Wolters and Gerald, 2008; Budetta, 2011; Styles, Coggan and Pine, 2011; Hastie *et al.*, 2021; Das and Chakraborty, 2022; López-Fernández *et al.*, 2022; Zhang *et al.*, 2023, 2024).

However, some differences in the failure mechanism can be observed between the two cliff types: while the highest cliff (model 1-h, Figure 5a) presents a clear shear band, joining the tip of the notch to the top of the cliff, and a tensile failure zone limited to a superficial portion of the cliff, the lowest cliff (model 5-h, Figure 5d) has a much wider shear band which affects a larger portion of the cliff, mostly concentrated at its top, and tensile failures occur throughout the entire slope height.. Therefore, it is possible to assess that:

- tension cracks on the cliff surface are more easily produced when the notch forms a rock column of low slenderness (i.e., stocky beam), where the slenderness is the ratio between the height of the cliff overhang and the length of the notch, $H_c/L_n$;
- the different failure mechanisms of the cliffs, due to a combined state of tensile, compressive and shear stresses that depend on the applied stress (in this case, the self-weight of the rock overhang), seem to be affected by the slenderness $H_c/L_n$. Specifically, the behaviour of the rock overhang moves from a prevalent tensile failure to a prevalent shear failure with increasing $H_c/L_n$, for a given $L_n$.

## 1. The back analysis of the 2014 rockfall event at Punta Ferruccio (Abruzzo, Italy)

Punta Ferruccio is a promontory located in Abruzzo Region (Italy). It is characterized by a 25 m high vertical cliffs on conglomerates with poorly cemented clayey sandstone and sandy clay interbedded layers and lenses (Figure 6). A basal notch on clayey deposits was present until 2014 and reached up to 7 m in depth and 4 m in height (Miccadei et al., 2019). A system of vertical joints spaced 3 to 10 m runs parallel to the cliff.

The most recent landslide affecting the promontory occurred in 2014 and consisted in a toppling failure in the eastern part of the cliff above a notch. Previous research, confirmed by repeated geomorphological surveys carried out from 2004 to 2017, demonstrated that the presence of notches as deep as 7 m and major joints parallel to the cliff extensively controlled the landslide phenomena on the cliff and its retreat (Miccadei et al., 2019). Therefore, in order to back analyse the 2014 landslide, a 2D FEM analysis was carried out by modifying the 1-h cliff model (Table

Accepted manuscript doi:
10.1680/jenge.24.00052

1) to include a vertical deep joint, in the position observed on site. The joint is modelled with the RS2 code with the first end (on the cliff surface) open and the last end closed. As shown in Figure 7, the discontinuity was located 7 m far from the exposed cliff face.

Since the persistence of the joint was unknown (as in most cases), the back analysis consisted in defining the joint persistence that provided a SRF around 1 (incipient collapse condition). The model was then used for parametric analyses aimed to investigate the effect of different persistences on the cliff stability and also the progressive degradation of the rock bridges.

Specifically, ten cliff models with joint persistence, $p$, from 100% up to 50% were generated. The different persistences were modelled by a correspondent reduction of the joint strength parameters (when the persistence is null, i.e., no joint, the strength characteristics along the joint are those of the rock), i.e. friction angle, $\varphi$, cohesion, $c$, and tensile strength, $\sigma_t$. As shown in Table 3, the equivalent mechanical properties assigned to the joint in each model were obtained from Eqs. (1)-(3), in order to take the presence of rock bridges into account:

$$\varphi = p\ \varphi_j + (1-p)\varphi_R \quad (1)$$

$$c = p\ c_j + (1-p)c_R \quad (2)$$

$$\sigma_t = p\ \sigma_{t\_j} + (1-p)\ \sigma_R \quad (3)$$

where $\varphi_j$, $c_j$ and $\sigma_{t\_j}$ represent the friction angle, cohesion and tensile strength of the joint, and $\varphi_R$, $c_R$ and $\sigma_{t\_R}$ the friction angle, cohesion and tensile strength of the rock, from Calista et al. (2019).

The first two models 1-PF and 2-PF (i.e. with a persistence of 100% and 65%, respectively) were unstable and the analyses did not reach convergence.

Models 3-PF and 4-PF, with a lower persistence, reached convergence but were unstable, while model 5-PF had a SRF = 1 and therefore its joint properties (p=62.4%, $\varphi_j$ =35.6°, $c_j$=149.1 kPa and $\sigma_{t\_j}$ = 142.9 kPa) were considered representative of the Punta Ferruccio cliff in-situ conditions before the 2014 rockfall event.

The results of this model, shown in Figure 8, demonstrate that the presence of a vertical deep joint located at a distance $d=L_n$ meters from the cliff face strongly influences the failure mode of the cliff. In fact, if compared to the results of the same model without the joint (i.e. homogeneous model 1-h shown in Figure 5), shear strains and yielded elements develop in a very limited portion of the cliff, close to the notch apex, while behind the vertical joint no effects can be detected. This behaviour, which results in a toppling failure mechanism, is clearly induced by the presence of the discontinuity (which constitutes a lateral release) and is even more evident from the total displacement results shown Figure 8b. This outcome is in agreement with Calista et al. (2019) findings.

Table 3 shows the critical SRFs of the eight cliff models with joints that reached convergence. As expected, the SRF increases as the joint persistence decreases, indicating that the cliff becomes more stable when a higher number (or extension) of rock bridges is present. Therefore, variations in the joint persistence affect the cliff stability in terms of critical SRF. However, no difference is provided in terms of failure mechanism, because the deep joint represents in all cases a surface release of the rock mass. Influence of the horizontal location of the vertical joint on the stability of cliffs with basal erosion

In order to investigate how cliff stability is influenced by the position of a deep vertical joint, the geometry of 5-PF cliff model (with the joint located 7 m far from the cliff face) was modified to simulate different joint locations. Specifically, new models with a joint at 4 m, 5.5 m, 8.5 m and 10 m far from the cliff face were generated and analysed.

As shown in Figure 9 and Figure 10, when the distance, *d*, between the joint and the cliff face is significantly lower than the notch depth (i.e., $d<L_n$), the joint has little influence on both the SRF and mechanical behaviour of the cliff. As illustrated in Figure 9a,b, and c, the failure mechanism of the cliff with the joint at 4 m from the cliff face is the same of that shown by the homogeneous model 1-h. On the contrary, as shown in Figure 8 and Figure 9d,e,f, if the joint is located at a distance from the cliff face almost equal or greater than the notch depth, its presence induces a significant perturbation that causes a reduction of the safety factor, more concentrated tensile failures at the top of the cliff (that may induce the development of tension cracks), shear strains localized in a smaller area close to the notch apex, larger displacements occurring only above the erosion area, and more diffuse yielded zones that affect also the exposed cliff face. When the structural joint (which can be considered as weakness plane in the rock cliff) is reached by the propagation of the notch and affected by the resulting stress concentration, it contributes to the collapse of the rock overhang, if its volume is sufficiently large. These findings are in good agreement with the results of Zhang et al. (2023), who analysed the failure process of a cliff with a tensile crack located directly above the notch apex.

Accepted manuscript doi:
10.1680/jenge.24.00052

## 2. Conclusions

Coastal erosion is generating great concern worldwide since they pose a significant threat to the safety of people, and cause damage to structures, infrastructures and coastal heritage with severe socio-economic implications.

The ongoing climate changes have intensified the occurrence of extreme atmospheric and oceanic events, leading to growing meteorological uncertainties, resulting in a loss of accuracy of traditional (empirical, history-based) methodologies for assessing coastal vulnerability. Coastal landslides are increasingly occurring due to the higher frequency-magnitude of storm surges, wave conditions, wind speed and sea level rise, since they are responsible for a more intense rock weathering and basal erosion (undermining and notching), especially in soft rock cliffs.

Therefore, coastal erosion prediction has become a major topic worldwide and a deeper understanding of the failure mechanisms of high coastal areas are required in order to more reliably assess coastal hazard. This is essential for management plans and coastal zone governance, as well as fundamental to identify and design appropriate stabilizing interventions.

To this aim, this research investigates how a basal notch growth influences the stability of homogeneous soft rock cliffs. The effect of the slenderness of the system cliff-notch on the mechanical disturbance is highlighted in terms of shear strain concentration, yielded areas and mechanism of instability. It has been found that the depth of the undermining plays a significant role on cliff stability, whose mechanism of collapse changes from a prevalent shear failure when

the cliff height is much greater than the notch depth to a prevalent tensile failure for low cliff heights. Moreover, a soft rock cliff affected by the presence of a vertical joint has been analysed with the aim to investigate the effects of the joint persistence and position (with respect to the cliff face) on the global stability of the cliff. The increasing of joint persistence can also represent the progressive deterioration of rock bridges mechanical characteristics over time due, for example, to the action of marine environment. The results obtained indicate that the higher is the persistence the lower is the global factor of safety, as expected. Moreover, for a given persistence, as the joint moves away from the cliff face the factor of safety decreases. The worse condition is represented by a discontinuity close to the notch end, since it represents a release of the rock mass and, consequently, the failure mechanism changes from a sliding to a toppling. Then, from a certain distance from the notch end, its negative influence reduces and the factor of safety starts increasing again.

In order to extend the results of this study, future research will (i) consider different cliff, joint and notch geometries and characteristics, (ii) resort to a FDEM (Finite-Discrete Element Method) code, in order to simulate the evolution of the failure processes and (iii) incorporate the effect of rock weathering in the numerical modelling, by properly reducing the mechanical parameters in the most exposed rock section.

**Acknowledgments**
This study was carried out within the RETURN Extended Partnership and received funding from the European Union Next-GenerationEU (National Recovery and Resilience Plan – NRRP, Mission 4, Component 2, Investment 1.3 – D.D. 1243 2/8/2022, PE0000005).

Accepted manuscript doi:
10.1680/jenge.24.00052

It was presented during the 2nd Mediterranean Symposium on Landslides, held in Hammamet (Tunisia) in October 2023.
The authors thank Povanat Inkate for his valuable collaboration.

**Notations**

$L_n$ is the notch depth

$H_n$ is the notch height

$H_c$ is the cliff height

E is the deformation Modulus of the rock

ν is the Poisson coefficient of the rock

c is the cohesion of the rock

φ is the friction angle of the rock

$\sigma_t$ is the tensile strength of the rock

$\varphi_j$ is the friction angle of the joint

$c_j$ is the cohesion of the joint

$\sigma_{t\_j}$ is the tensile strength of the joint

SF is the safety factor of the cliff

SRF is the strength reduction factor

p is the persistence of the joint

d is the distance of the joint from the cliff face

**References**

Andriani, G. and Pellegrini, V. (2014) 'Qualitative assessment of the cliff instability susceptibility at a given scale with a new multidirectional method', *International Journal of Geology*, 8, pp. 73–80.

Bonaldo, D. *et al.* (2019) 'Integrating multidisciplinary instruments for assessing coastal vulnerability to erosion and sea level rise : lessons and challenges from the Adriatic Sea, Italy', *ournal of Coastal Conservation*, 23, pp. 19–37. doi:https://doi.org/10.1007/s11852-018-0633-x.

Bray, M.J. and Hooke, J.M. (1997) 'Prediction of soft-cliff retreat with accelerating sea-level rise', *Journal of Coastal Research*, 13(2), pp. 453–467.

Budetta, P. (2011) 'Stability of an undercut sea-cliff along a Cilento coastal stretch (Campania, Southern Italy)', *Natural Hazards*, 56, pp. 233–250. doi:10.1007/s11069-010-9565-y.

Budetta, P., Santo, A. and Vivenzio, F. (2008) 'Landslide hazard mapping along the coastline of the Cilento region (Italy) by means of a GIS-based parameter rating approach', *Geomorphology*, 94, pp. 340–352. doi:10.1016/j.geomorph.2006.10.034.

Calista, M. *et al.* (2019) 'Recent geomorphological evolution and 3d numerical modelling of soft clastic rock cliffs in the mid-western adriatic sea (Abruzzo, italy)', *Geosciences (Switzerland)*, 9(7). doi:10.3390/geosciences9070309.

Castedo, R. *et al.* (2017) 'The Modelling of Coastal Cliffs and Future Trends', in *Hydro-Geomorphology - Models and Trends*. Dericks P. INTECH, pp. 53–78. doi:10.5772/intechopen.68445.

Das, S. and Chakraborty, D. (2022) 'Effect of undercut on the lower bound stability of vertical rock escarpment using finite element and power cone programming', *Front. Struct. Civ. Eng.*, 16(8), pp. 1040–1055. doi:https://doi.org/10.1007/s11709-022-0841-1.

Dickson, M.E., Walkden, M.J.A. and Hall, J.W. (2007) 'Systemic impacts of climate change on an eroding coastal region over the twenty-first century', *Climatic Change*, 84(2), pp. 141–166. doi:10.1007/s10584-006-9200-9.

Dodge-Wan, D. Nagarajan, R. (2019) 'Typology and Mechanisms of Coastal Erosion in Siliciclastic Rocks of the Northwest Borneo Coastline (Sarawak, Malaysia): A Field Approach', in *Coastal Zone Management : Global Perspectives, Regional Processes, Local Issues* -

*Shoreline and Coastal Changes*. Elsevier, pp. 65–98.

Duperret, A. *et al.* (2004) 'Coastal chalk cliff instability in NW France: Role of lithology, Fracture pattern and rainfall', *Geological Society, London, Engineering Geology Special Publications*, 20, pp. 33–55. doi:10.1144/GSL.ENG.2004.020.01.03.

Gerivani, H., Stephenson, W. and Afarin, M. (2020) 'Sea cliff instability hazard assessment for coastal management in Chabahar, Iran', *Journal of Coastal Conservation*, 24(1). doi:10.1007/s11852-019-00726-7.

Gómez-Pazo, A., Pérez-Alberti, A. and Trenhaile, A. (2021) 'Tracking the behavior of rocky coastal cliffs in northwestern Spain', *Environmental Earth Sciences*, 80(22), pp. 1–18. doi:10.1007/s12665-021-09929-4.

Hastie, W.W. *et al.* (2021) 'Linking fracturing and rock mechanic properties to the erosion of a beachrock shore platform', *Marine Geology*, 441, p. 106616. doi:10.1016/j.margeo.2021.106616.

Kline, S.W., Adams, P.N. and Limber, P.W. (2014) 'Geomorphology The unsteady nature of sea cliff retreat due to mechanical abrasion, failure and comminution feedbacks', *Geomorphology*, 219, pp. 53–67. doi:10.1016/j.geomorph.2014.03.037.

Kogure, T. *et al.* (2006) 'Effect of the development of notches and tension cracks on instability of limestone coastal cliffs in the Ryukyus, Japan', *Geomorphology*, 80(3–4), pp. 236–244. doi:10.1016/j.geomorph.2006.02.012.

Lollino, P. *et al.* (2018) 'FDEM analysis of fracturing processes affecting vertical cliffs in soft calcarenites', in *52nd U.S. Rock Mechanics/Geomechanics Symposium - ARMA*. Seattle, Washington, June 2018, p. 7.

Lollino, P. *et al.* (2021) 'Multi-scale approach to analyse the evolution of soft rock coastal cliffs and role of controlling factors: a case study in South-Eastern Italy', *Geomatics, Natural Hazards and Risk*, 12(1), pp. 1058–1081. doi:10.1080/19475705.2021.1910351.

López-Fernández, C. *et al.* (2022) 'Instability mechanisms and evolution of a rocky cliff on the Atlantic coast of Spain', *Journal of Coastal Conservation*, 26(60). doi:10.1007/s11852-022-00907-x.

Marques, F. (2018) 'Regional scale sea cliff hazard assessment at sintra and cascais counties, western coast of Portugal', *Geosciences (Switzerland)*, 8(3), pp. 1–22.

doi:10.3390/geosciences8030080.

Marques, F., Matildes, R. and Redweik, P. (2011) 'Statistically based sea cliff instability hazard assessment of Burgau- Lagos coastal section ( Algarve, Portugal )', *Journal of Coastal Research. Proceedings of the 11th International Coastal Symposium*, (64), pp. 927–931.

Miccadei, E. *et al.* (2019) 'Geomorphology of soft clastic rock coasts in the mid-western Adriatic Sea (Abruzzo, Italy)', *Geomorphology*, 324, pp. 72–94. doi:10.1016/j.geomorph.2018.09.023.

Naylor, L.A. and Stephenson, W.J. (2010) 'On the role of discontinuities in mediating shore platform erosion', *Geomorphology*, 114, pp. 89–100. doi:10.1016/j.geomorph.2008.12.024.

Nunes, M. *et al.* (2009) 'Hazard assessment in rock cliffs at Central Algarve (Portugal): A tool for coastal management', *Ocean and Coastal Management*, 52(10), pp. 506–515. doi:10.1016/j.ocecoaman.2009.08.004.

Pang, T. *et al.* (2023) 'Coastal erosion and climate change: A review on coastal-change process and modeling', *Ambio*, 52, pp. 2034–2052. doi:10.1007/s13280-023-01901-9.

De Pippo, T. *et al.* (2008) 'Coastal hazard assessment and mapping in Northern Campania, Italy', *Geomorphology*, 97(3–4), pp. 451–466. doi:10.1016/j.geomorph.2007.08.015.

Del Río, L. and Gracia, F.J. (2009) 'Erosion risk assessment of active coastal cliffs in temperate environments', *Geomorphology*, 112(1–2), pp. 82–95. doi:10.1016/j.geomorph.2009.05.009.

Ružić, I. *et al.* (2015) 'A stability assessment of coastal cliffs using digital imagery', *Acta Geotechnica Slovenica*, 12(2), pp. 25–35.

Styles, T.D., Coggan, J.S. and Pine, R.J. (2011) 'Back analysis of the Joss Bay Chalk Cliff Failure using numerical modelling', *Engineering Geology*, 120(1–4), pp. 81–90. doi:10.1016/j.enggeo.2011.04.004.

Sunamura, T. (1975) 'A laboratory study of wave-cut platform formation', *Journal of Geology*, 83, pp. 389–397.

Sunamura, T. (2015) 'Rocky coast processes: With special reference to the recession of soft rock cliffs', *Proceedings of the Japan Academy Series B: Physical and Biological Sciences*, 91(9), pp. 481–500. doi:10.2183/pjab.91.481.

Theodore, P. *et al.* (2020) 'Erosion status of a sea cliff promontory bounding an ecologically important beach', *Journal of Coastal Conservation*, 24(19). doi:10.1007/s11852-020-00756-6.

Wolters, G. and Gerald, M. (2008) 'Effect of Cliff Shape on Internal Stresses and Rock Slope Stability', *Journal of Coastal Research*, 24(1), pp. 43–50. doi:10.2112/05-0569.1.

Young, A.P. (2018) 'Decadal-scale coastal cliff retreat in southern and central California', *Geomorphology*, 300, pp. 164–175. doi:https://doi.org/10.1016/j.geomorph.2017.10.010.

Young, A.P. *et al.* (2021) 'Three years of weekly observations of coastal cliff erosion by waves and rainfall', *Geomorphology*, 375(107545). doi:10.1016/j.geomorph.2020.107545.

Young, A.P. and Ashford, S.A. (2008) 'Instability investigation of cantilevered seacliffs', *Earth Surface Processes and Landforms*, 33, pp. 1661–1677. doi:10.1002/esp.1636.

Zhang, Q. *et al.* (2023) 'Investigation of the stability and failure mechanism of slopes in Xiyu conglomerate due to toe erosion', *Bulletin of Engineering Geology and the Environment*, 82(206). doi:10.1007/s10064-023-03225-0.

Zhang, Q. *et al.* (2024) 'Centrifuge modeling test on reactivation of ancient landslide under sudden drop of reservoir water and rainfall', *Acta Geotechnica* [Preprint]. doi:10.1007/s11440-023-02217-4.

Accepted manuscript doi:
10.1680/jenge.24.00052

**Tables**

Table 1 Input parameters for cliff stability analyses (Calista *et al.*, 2019). E and ν: deformation Modulus and Poisson coefficient of the rock; c and φ: Mohr-Coulomb parameters of the rock; $\sigma_t$: tensile strength of the rock

| E [MPa] | ν [-] | γ [kN/m$^3$] | c [kPa] | φ [°] | $\sigma_t$ [MPa] |
|---|---|---|---|---|---|
| 240 | 0.3 | 21 | 380 | 45 | 0.38 |

Table 2 Results of the 2D FEM analyses – homogeneous cliff models with variable $H_c$, $L_n$ = 7 m, and $h_n$ = 4 m

| Model | Cliff height, $H_c$ [m] | Slenderness $H_c/L_n$ | SRF |
|---|---|---|---|
| 1-h | 25 | 3.6 | 2.12 |
| 2-h | 20 | 2.9 | 2.21 |
| 3-h | 15 | 2.1 | 2.32 |
| 4-h | 10 | 1.4 | 2.24 |
| 5-h | 7 | 1.0 | 1.93 |

Accepted manuscript doi:
10.1680/jenge.24.00052

Table 3 RS2 results for the 10 Punta Ferruccio (PF) models analysed, with $H_c$ = 25 m, joint length = 23.75 m, $L_n$ = 7 m, and $h_n$ = 4 m. □φ, □c and □$\sigma_t$ indicate the increase in the joint parameters (φ, c and $\sigma_t$, respectively) with the decreasing of persistence from 100% to p.

| Model | p [%] | φ [°] | □φ [%] | c [kPa] | □c [%] | $\sigma_t$ [kPa] | □$\sigma_t$ [%] | SRF |
|---|---|---|---|---|---|---|---|---|
| 1-PF | 100 | 30 | 0.00 | 10 | 0.0 | 38 | 0.0 | unknown |
| 2-PF | 65 | 35.3 | 0.18 | 139.5 | 13.0 | 157.7 | 3.15 | unknown |
| 3-PF | 63 | 35.6 | 0.19 | 146.9 | 13.7 | 164.5 | 3.33 | 0.35 |
| 4-PF | 62.5 | 35.6 | 0.19 | 148.8 | 13.9 | 166.3 | 3.38 | 0.98 |
| **5-PF** | **62.4** | **35.6** | **0.19** | **149.1** | **13.9** | **166.6** | **3.38** | **1** |
| 6-PF | 62.3 | 35.7 | 0.19 | 149.5 | 13.9 | 166.9 | 3.39 | 1.15 |
| 7-PF | 62 | 35.7 | 0.19 | 150.6 | 14.1 | 168.0 | 3.42 | 1.28 |
| 8-PF | 61.5 | 35.8 | 0.19 | 152.5 | 14.2 | 169.7 | 3.47 | 1.38 |
| 9-PF | 60 | 36.0 | 0.20 | 158.0 | 14.8 | 174.8 | 3.60 | 1.74 |
| 10-PF | 50 | 37.5 | 0.25 | 195 | 18.5 | 209 | 4.50 | 2.07 |

Accepted manuscript doi:
10.1680/jenge.24.00052

**Figure captions**

Figure 1. Location of Punta Ferruccio, Italy (Google Earth Map Data, Dat SIO NOAA, U.S. Navy, NGA, GEBCO, Image ®2023 TerraMetrics, Image Landsat/Copernicus)

Figure 2 Example of a homogeneous cliff model in RS2, with a height of 25 m ($H_c$), and a basal notch 7 m deep ($L_n$) and 4 m high ($h_n$). Two excavation processes, named "Excavation area" and "Notch", are simulated to avoid stress modelling disturbance

Figure 3. Notch growth for the 25 m high cliff (only a part of the cliff above the erosion area is visible, since the more superficial zone does not experience shear concentrations and yielding): maximum shear strains and yielded elements. Pictures a)-g) show the different excavation stages

Figure 4. Notch growth for the 7 m high cliff: maximum shear strains and yielded elements. Pictures a)-g) show the different excavation stages

Figure 5. Maximum shear strains, total displacements and yielded elements at failure of models 1-h (a), b) and c), respectively) and 5-h (d), e) and f), respectively)

Figure 6. Lithological and geomorphological setting of Punta Ferruccio coastal cliff, made on conglomerate (cg), with basal notch in sandy-clay (sc) and joints (j). The picture shows the notch before the topple event of 2014. Behind, the deposits of the rockfall event occurred on 2004-2005 (rf) triggered by at that time northwards extension of the basal notch (from Miccadei et al., 2019, modified)

Figure 7. Punta Ferruccio cliff model in RS2

Figure 8. Results of model 5-PF. a) Maximum shear strains and deformation vectors (arrows); b) total displacements; c) yielded elements

Figure 9. Results of the cliff models with a deep vertical joint located at different distances, d, from the cliff face. a, b, c) maximum shear strains, total displacements and yielded elements, respectively, when d= 4m; d, e, f) maximum shear strains, total displacements and yielded elements, respectively, when d= 10 m

Figure 10. SRFs of sea cliff models with different horizontal locations of the vertical joint

Accepted manuscript doi:
10.1680/jenge.24.00052

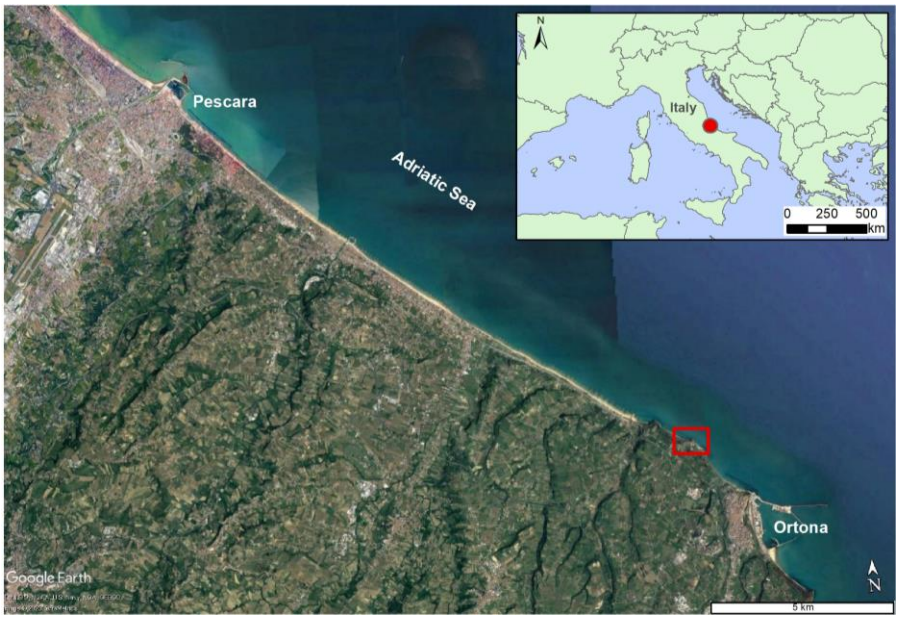


Fig. 1

Accepted manuscript doi:
10.1680/jenge.24.00052

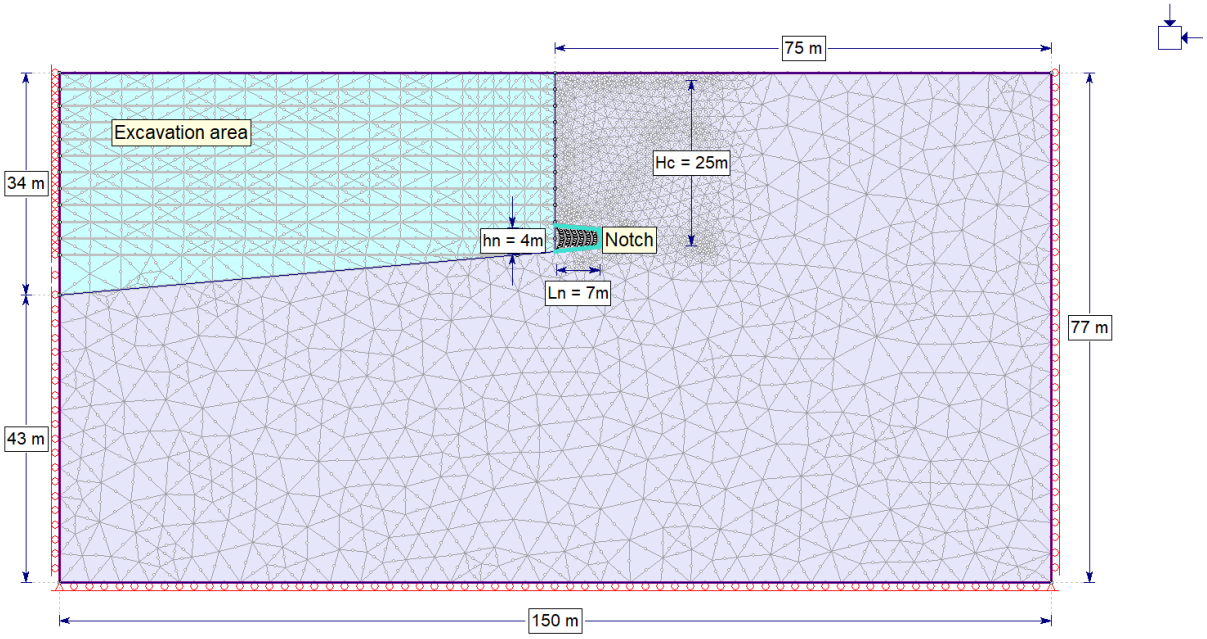


Fig. 2

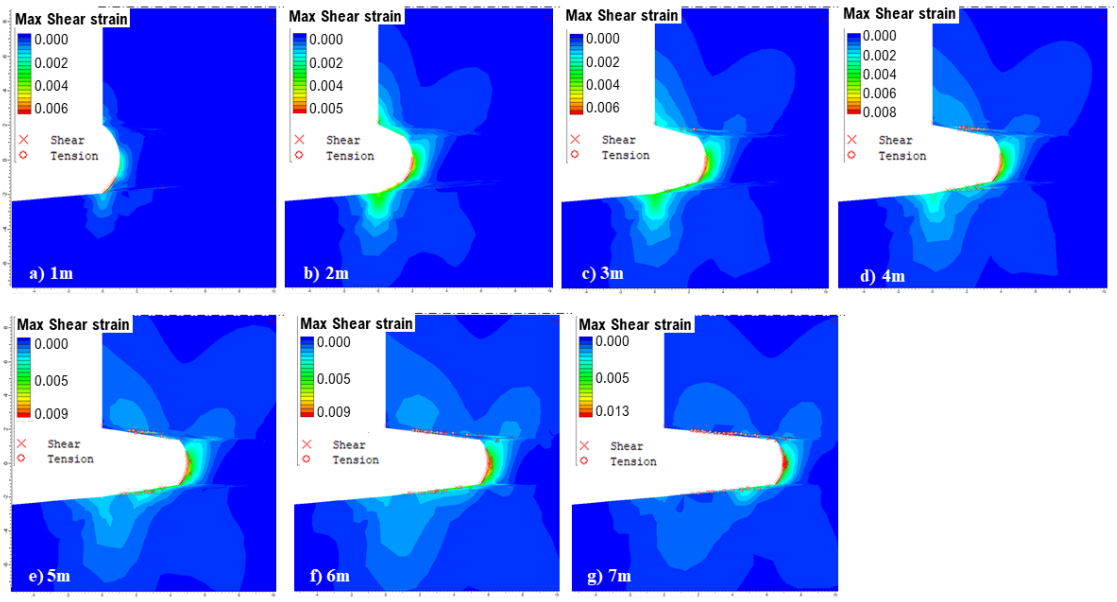


Fig. 3

Accepted manuscript doi:
10.1680/jenge.24.00052

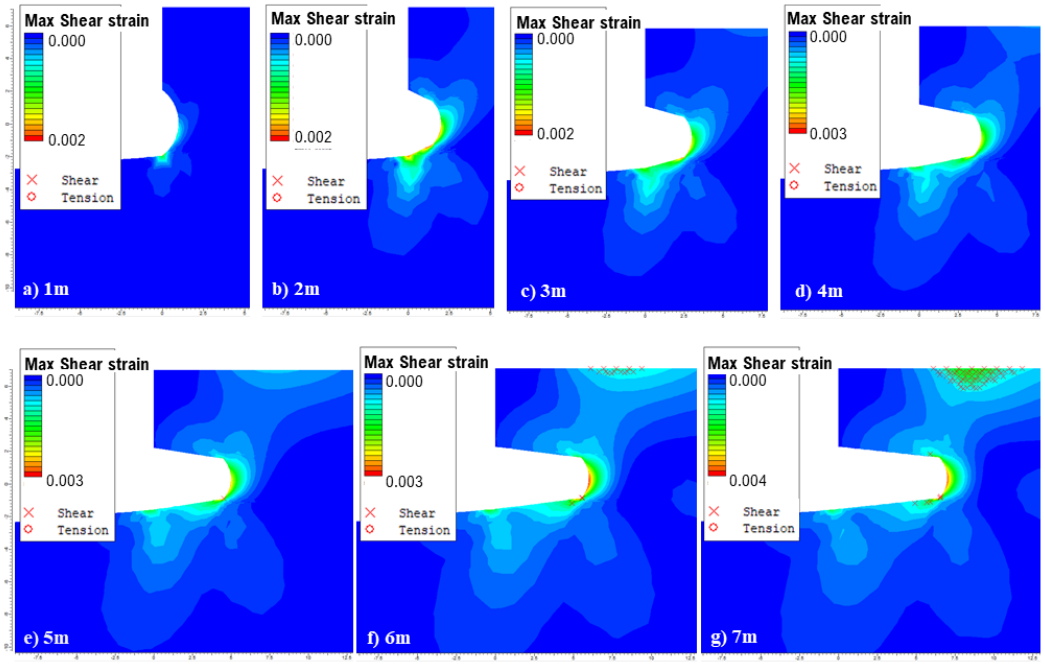


Fig. 4

Accepted manuscript doi:
10.1680/jenge.24.00052

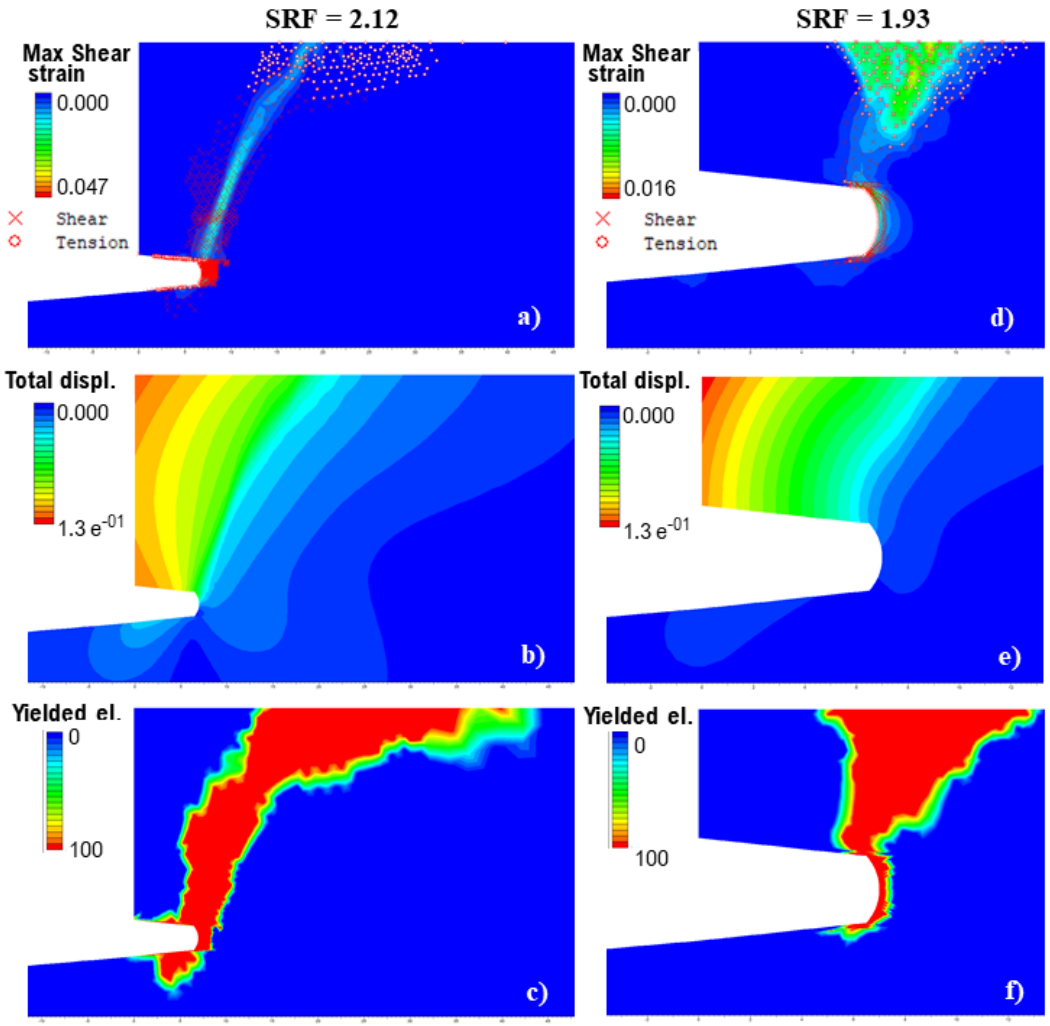


Fig. 5

Accepted manuscript doi:
10.1680/jenge.24.00052

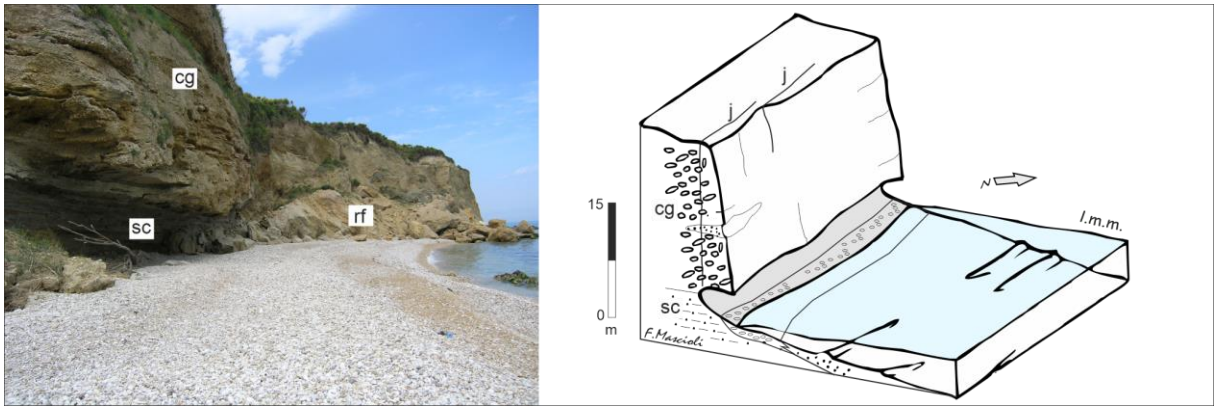


Fig. 6

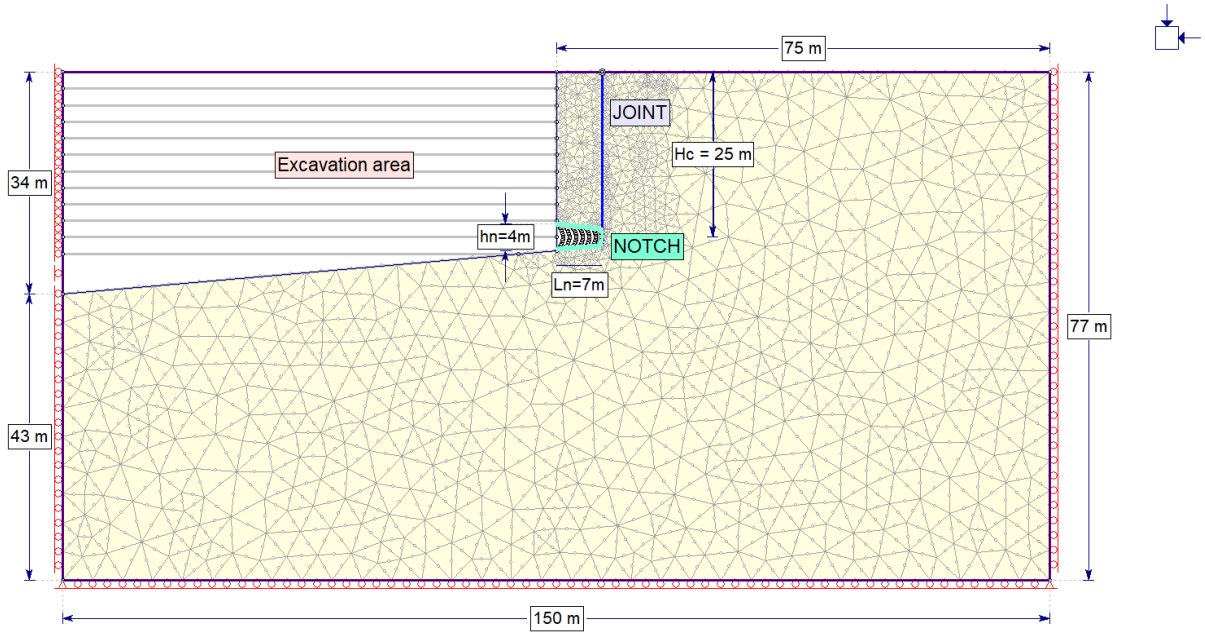


Fig .7

Accepted manuscript doi:
10.1680/jenge.24.00052

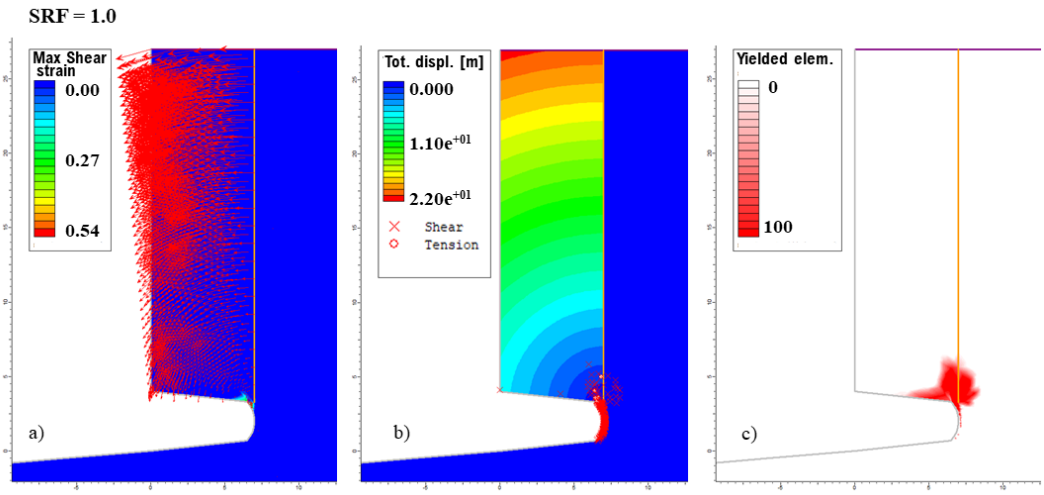


Fig. 8

Accepted manuscript doi:
10.1680/jenge.24.00052

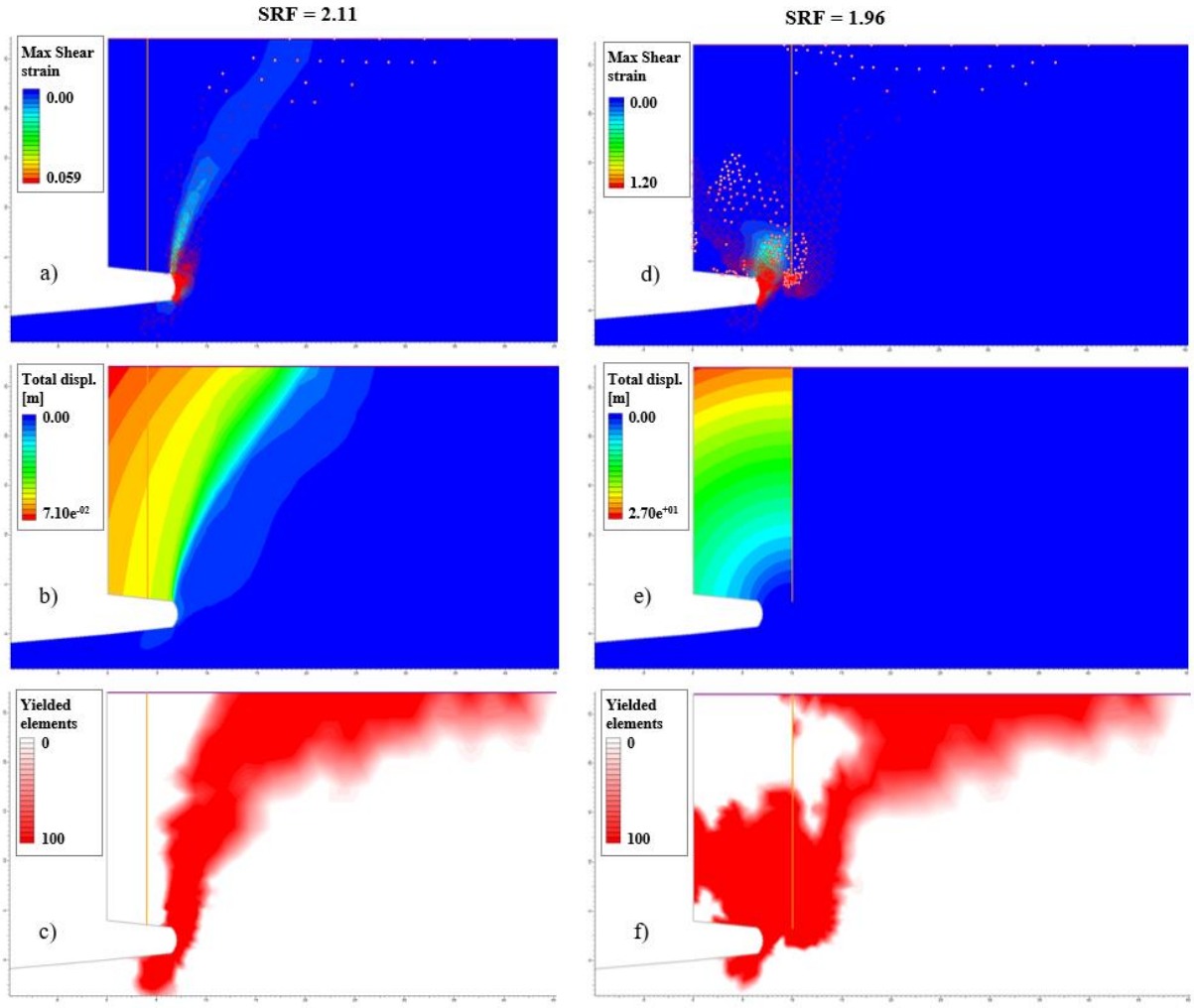


Fig. 9

| Model | Joint distance from the cliff face, d [m] | SRF [-] | Ref. Figure |
|---|---|---|---|
| 5-PF_J4m | 4 | 2.11 | Fig. 9a,b,c |
| 5-PF_J5.5m | 5.5 | 1.92 | - |
| 5-PF | 7 | 1 | Fig. 8a,b,c |
| 5-PF_J8.5m | 8.5 | 1.81 | - |
| 5-PF_J10m | 10 | 1.96 | Fig. 9d,e,f |

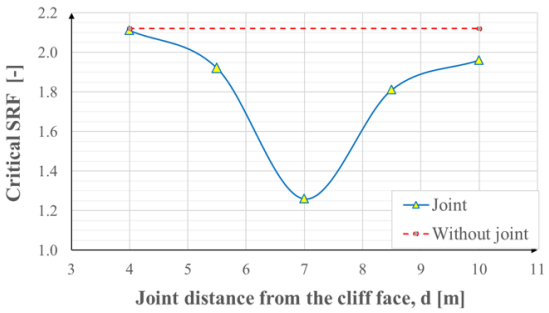


Fig. 10